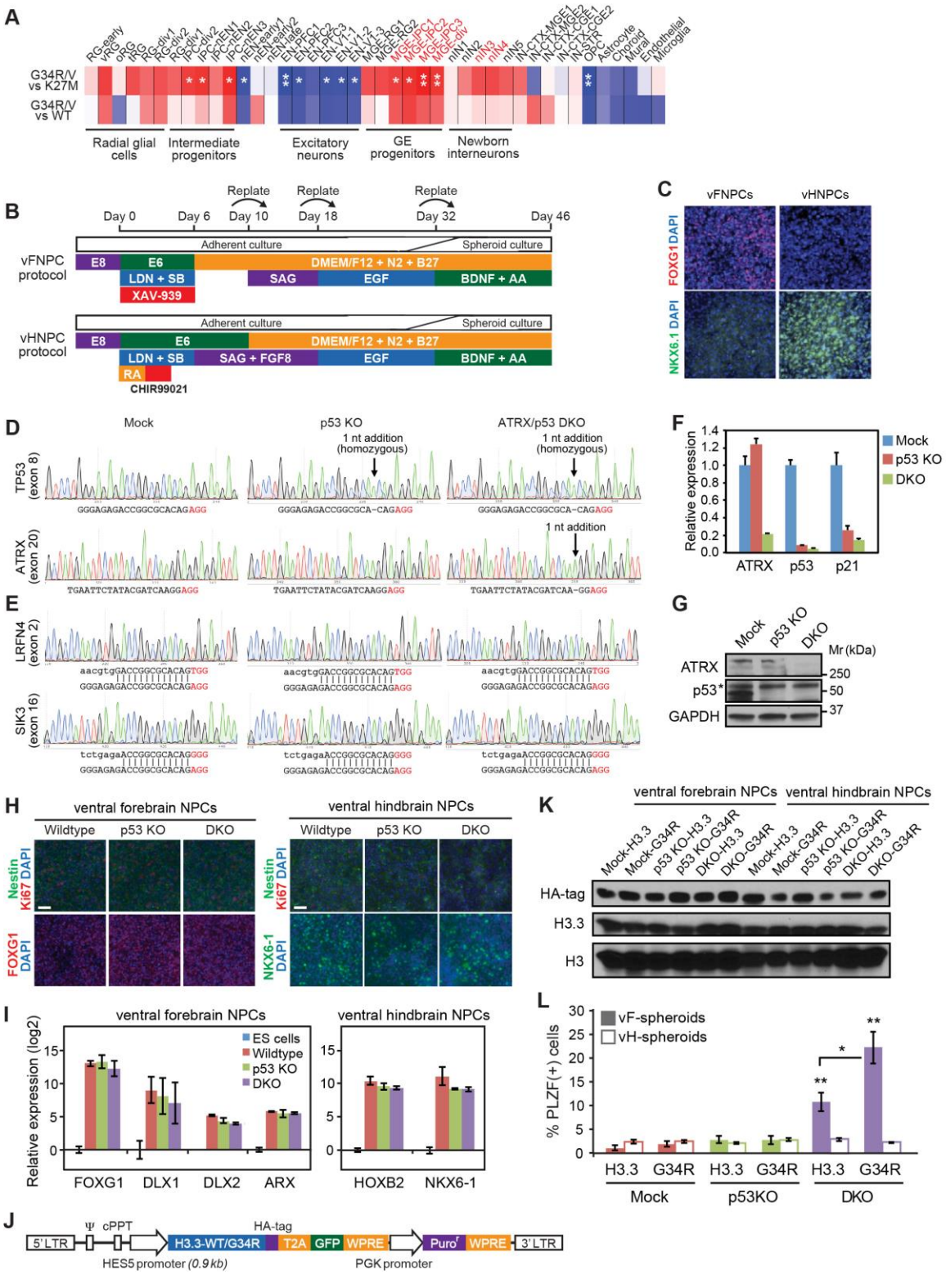
A
G34R/V vs K27M
G34R/V vs WT
Radial glial cells
Intermediate progenitors
Excitatory neurons
GE progenitors
Newborn interneurons
B
Day 0
Day 6
Day 10
Day 18
Day 32
Day 46
Replate
Adherent culture
Spheroid culture
vFNPC protocol
vHNPC protocol
E8
E6
LDN + SB
XAV-939
SAG
SAG + FGF8
EGF
BDNF + AA
DMEM/F12 + N2 + B27
RA
CHIR99021
C
vFNPCs
vHNPCs
FOXG1 DAPI
NKX6.1 DAPI
D
Mock
p53 KO
ATRX/p53 DKO
1 nt addition (homozygous)
1 nt addition
TP53 (exon 8)
ATRX (exon 20)
E
LRFN4 (exon 2)
SIK3 (exon 16)
F
Relative expression
Mock
p53 KO
DKO
ATRX
p53
p21
G
Mock
p53 KO
DKO
Mr (kDa)
ATRX
p53*
GAPDH
250
50
37
H
ventral forebrain NPCs
ventral hindbrain NPCs
Wildtype
p53 KO
DKO
Nestin Ki67 DAPI
FOXG1 DAPI
NKX6-1 DAPI
I
ventral forebrain NPCs
ventral hindbrain NPCs
Relative expression (log2)
ES cells
Wildtype
p53 KO
DKO
FOXG1
DLX1
DLX2
ARX
HOXB2
NKX6-1
J
Ψ
cPPT
HA-tag
5' LTR
H3.3-WT/G34R
T2A
GFP
WPRE
Puro'
WPRE
3' LTR
HES5 promoter (0.9 kb)
PGK promoter
K
ventral forebrain NPCs
ventral hindbrain NPCs
Mock-H3.3
Mock-G34R
p53 KO-H3.3
p53 KO-G34R
DKO-H3.3
DKO-G34R
HA-tag
H3.3
H3
L
vF-spheroids
vH-spheroids
% PLZF(+) cells
H3.3
G34R
Mock
p53KO
DKO

Figure S1. Characterization of tumor model cells, related to Figure 1.
(A) Heatmap shows enrichment (red) and depletion (blue) of expression signatures extracted from the indicated cell populations described in Nowakowski *et al*. *P* values were calculated by random permutation of sample labels (n = 1,000) and adjusted for multiple comparisons. (B) Schematic illustration of differentiation protocols for vFNPCs (upper) and vHNPCs (lower). (C) Immunohistochemistry for forebrain marker FOXG1 and hindbrain marker NKX6.1 demonstrates their cell type-specific expression. (D) Mutations created by CRISPR/Cas9 gene editing were validated by Sanger sequencing of genomic DNA. Nucleotide sequences of guide RNAs are shown below. Red letters indicate the PAM sequence (NGG). (E) Sanger sequencing of genomic DNA shows that putative off-targets sites are unaffected. (F) RT-qPCR demonstrates the decreased expression of knocked-out genes and p53 target gene p21. Bars indicate mean ± S.E.M. (n = 3). (G) Western blotting confirmed the loss of expression of ATRX and p53. Asterisk indicates unspecific bands. (H) At day 18 of differentiation, vFNPCs and vHNPCs were immunostained with the indicated antibodies and counterstained with DAPI. Scale bar, 20 μm. (I) RT-qPCR shows the expression of interneuron markers and hindbrain markers in each cell type. Bars indicate mean ± S.E.M. (n = 3). (J) Schematic illustration of H3.3-expressing construct. (K) Western blotting of chromatin fraction shows the expression of histone H3.3 transgenes and incorporation into chromatin. (L) Intracellular flow cytometry shows an increase of PLZF-positive early neuroectoderm cells in the ventral forebrain (vF) cultures but not in ventral hindbrain (vH) cultures. Bars indicate mean ± S.E.M. (n = 4-5). *P* values in panel (L) were calculated by two-sided Welch's t test. **P* < 0.05, ***P* < 0.01.

A

Mutations	Cell type	# of animals that reached the humane endpoint at 6 months	Median survival (days)
DKO + H3.3G34R + MYCN	Forebrain	8/8 (100%)	99.5
DKO + H3.3WT + MYCN	Forebrain	3/8 (37.5%)	>172.5
DKO + H3.3G34R + MYCN	Hindbrain	0/7 (0%)	-
DKO + H3.3G34R	Forebrain	1/8 (12.5%)	-
DKO + H3.3WT	Forebrain	0/8 (0%)	-
DKO + H3.3G34R	Hindbrain	0/5 (0%)	-
Mock NPCs	Forebrain	0/3 (0%)	-

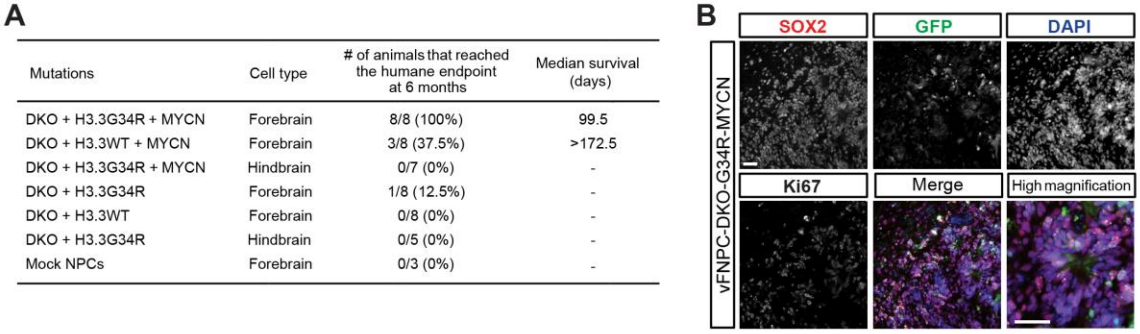

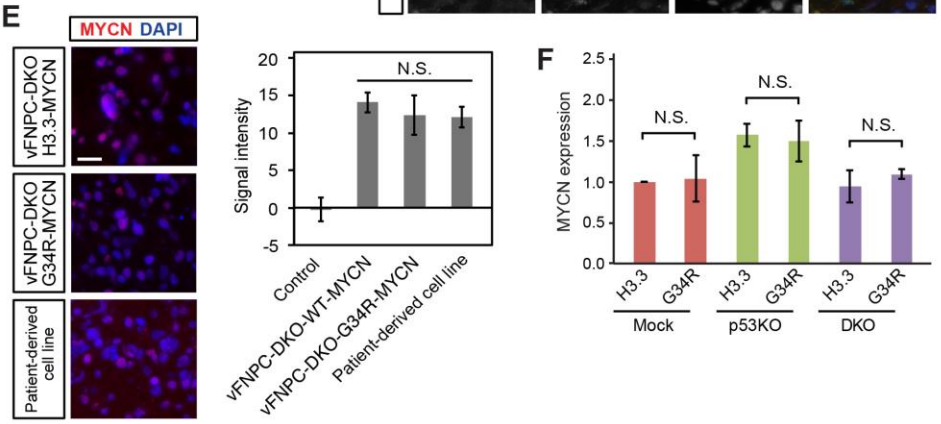

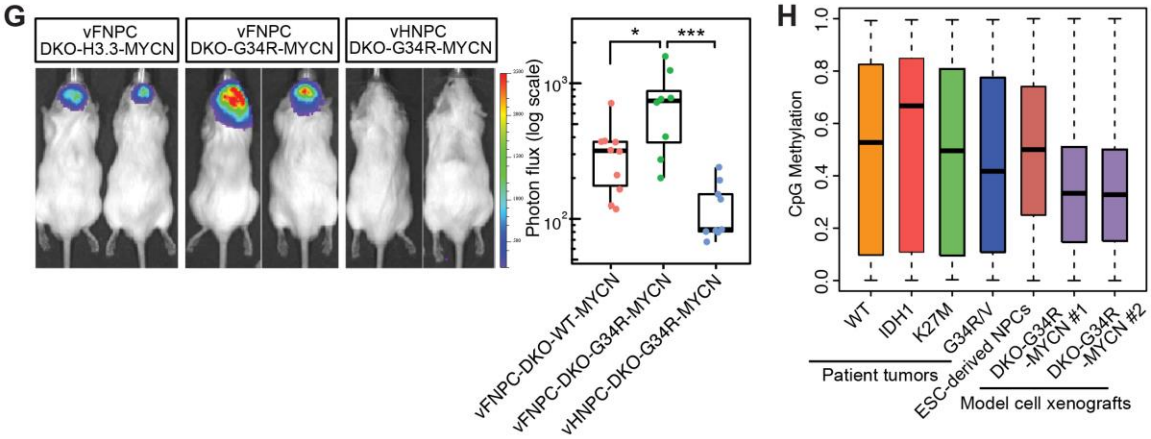

Figure S2. Characterization of xenografts, related to Figure 2.
(A) Summary of *in vivo* tumorigenicity assays. Mutation status and type of cells transplanted intracranially in NOD/SCID mice, and survival outcomes are shown. DKO: ATRX/TP53 double knockout, NPCs: Neural Progenitor Cells. (B) Frozen section of mouse brain transplanted with the quadruple-mutant cells (vFNPC-DKO-G34R-NMYC) was immunostained for SOX2 and Ki67. High-magnification image shows a representative rosette structure. Scale bar, 20 μm. (C) DAB-staining for human NCAM shows leptomeningeal spread of transplanted cells. (D) Immunohistochemistry shows the maintained expression of interneuron markers in transplanted cells. Scale bar, 20 μm. (E) Immunostaining for N-Myc shows similar expression levels in xenografts. Scale bar, 20 μm. Signal intensity was calculated using Image J. Brain sections of non-grafted animals were used as control. Bars indicate mean ± S.E.M. (n = 4). (F) RT-qPCR shows that H3.3G34R mutation does not affect the expression of N-Myc in vFNPCs. Bars indicate mean ± S.E.M. (n = 4). (G) Intracranial growth of luciferase-labeled cells was measured by quantitative *in vivo* bioluminescence imaging. (n = 8-10) (H) Boxplot shows CpG methylation levels of the indicated groups. Each human patient tumor subtype consists of 4 samples. *P* values were calculated by two-sided Welch's t test (E, F) or by Wilcoxon rank-sum test (G). $*P < 0.05$, $***P < 0.001$. NS, Not Significant.

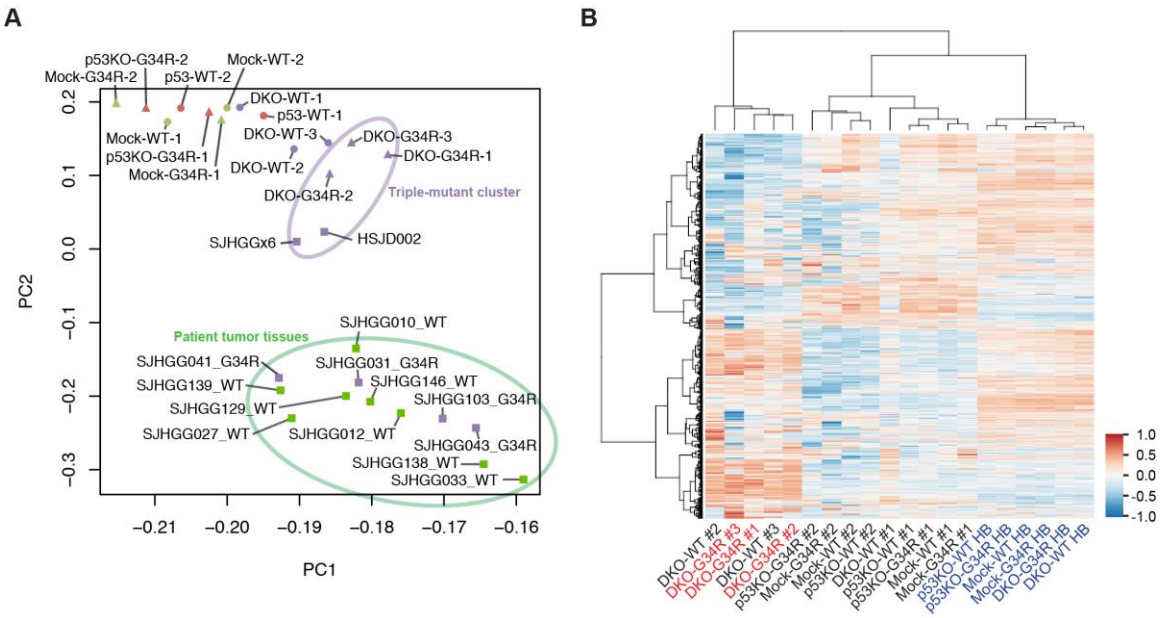

Figure S3. Hierarchical clustering of RNA-seq data, related to Figure 3.
(A) Principal Component Analysis of RNA-seq data from the tumor model cells, H3.3G34R-mutant patient-derived cell lines (SJHGGx6 and HSJD002), and patient tumor tissues (St Jude's dataset, green). (B) Unsupervised hierarchical clustering of RNA-seq data. HB: Hindbrain. The remaining groups are all forebrain in origin.

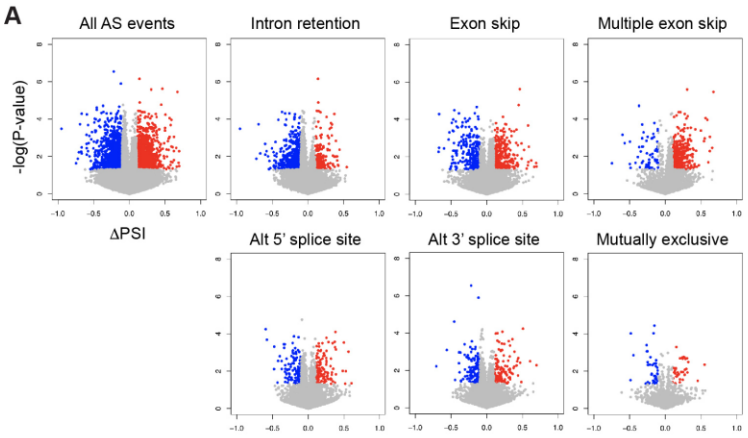

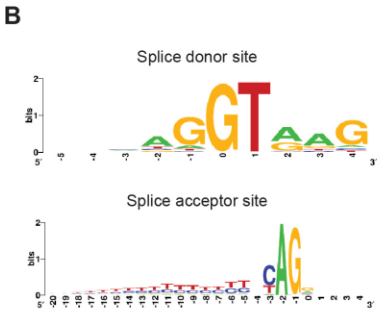

C

Upregulated AS (All)

Category	Term	Count	%	P-Value	Benjamini
UP_KEYWORDS	Alternative splicing	723	74.6	1.50E-64	6.00E-62
UP_KEYWORDS	Phosphoprotein	601	62	3.80E-54	7.80E-52
UP_SEQ_FEATURE	splice variant	564	58.2	3.60E-45	8.80E-42
UP_KEYWORDS	Nucleus	378	39	1.90E-25	2.60E-23
UP_KEYWORDS	Cytoplasm	349	36	2.20E-23	2.30E-21
GOTERM_MF_DIRECT	protein binding	551	56.9	8.80E-18	7.70E-15
GOTERM_CC_DIRECT	nucleoplasm	229	23.6	2.70E-17	1.50E-14
UP_KEYWORDS	Coiled coil	231	23.8	1.80E-16	1.80E-14
GOTERM_CC_DIRECT	cytoplasm	358	36.9	8.00E-15	2.30E-12
GOTERM_BP_DIRECT	G2/M transition of mitotic cell cycle	30	3.1	2.60E-11	7.10E-08

Downregulated AS (All)

Category	Term	Count	%	P-Value	Benjamini
UP_KEYWORDS	Alternative splicing	654	73.8	8.30E-59	3.30E-56
UP_KEYWORDS	Phosphoprotein	545	61.5	7.00E-50	1.40E-47
UP_SEQ_FEATURE	splice variant	519	58.6	6.40E-44	1.50E-40
UP_KEYWORDS	Cytoplasm	309	34.9	2.50E-19	3.30E-17
UP_KEYWORDS	Coiled coil	218	24.6	3.10E-18	3.10E-16
GOTERM_MF_DIRECT	protein binding	497	56.1	2.30E-17	1.90E-14
GOTERM_CC_DIRECT	cytoplasm	328	37	1.40E-15	7.90E-13
UP_KEYWORDS	Acetylation	214	24.2	2.70E-11	2.10E-09
GOTERM_CC_DIRECT	nucleoplasm	185	20.9	6.20E-10	1.70E-07
UP_KEYWORDS	Cytoskeleton	88	9.9	1.00E-08	6.60E-07

Upregulated AS (IR)

Category	Term	Count	%	P-Value	Benjamini
UP_KEYWORDS	Alternative splicing	117	66.5	2.20E-08	5.10E-06
UP_KEYWORDS	Phosphoprotein	97	55.1	1.70E-07	2.00E-05
UP_KEYWORDS	Nucleus	69	39.2	1.40E-06	1.10E-04
UP_SEQ_FEATURE	splice variant	89	50.6	5.10E-06	3.00E-03
GOTERM_CC_DIRECT	nucleoplasm	44	25	3.40E-05	7.50E-03
GOTERM_CC_DIRECT	nucleus	69	39.2	7.60E-05	8.50E-03
UP_KEYWORDS	Acetylation	45	25.6	3.10E-04	1.80E-02
UP_KEYWORDS	Cytoplasm	57	32.4	4.90E-04	2.30E-02
GOTERM_MF_DIRECT	protein binding	87	49.4	1.10E-03	2.70E-01
GOTERM_MF_DIRECT	poly(A) RNA binding	20	11.4	1.10E-03	1.50E-01
GOTERM_CC_DIRECT	spliceosomal complex	6	3.4	1.20E-03	8.40E-02

Downregulated AS (IR)

Category	Term	Count	%	P-Value	Benjamini
UP_KEYWORDS	Alternative splicing	321	71	2.40E-24	7.70E-22
UP_SEQ_FEATURE	splice variant	248	54.9	2.30E-16	2.80E-13
UP_KEYWORDS	Phosphoprotein	251	55.5	3.80E-15	6.30E-13
GOTERM_MF_DIRECT	protein binding	238	52.7	8.60E-07	4.60E-04
GOTERM_CC_DIRECT	nucleoplasm	96	21.2	1.90E-06	6.70E-04
UP_KEYWORDS	Coiled coil	96	21.2	1.70E-05	1.90E-03
UP_KEYWORDS	Cytoplasm	137	30.3	3.10E-05	2.50E-03
UP_KEYWORDS	Nucleus	146	32.3	4.30E-05	2.80E-03
GOTERM_CC_DIRECT	cytoplasm	149	33	5.30E-05	9.20E-03
UP_KEYWORDS	Methyltransferase	14	3.1	2.00E-04	1.10E-02

D

	H3.3G34R-mutant	Histone wildtype
Number of patients	4	8
Grade	IV (4/4)	IV (8/8)
Location	Hemisphere (4/4)	Hemisphere (8/8)
Sex	Female 2, Male 2	Female 4, Male 4
Mean age (Median age)	14.85 (14.41)	14.12 (13.96)

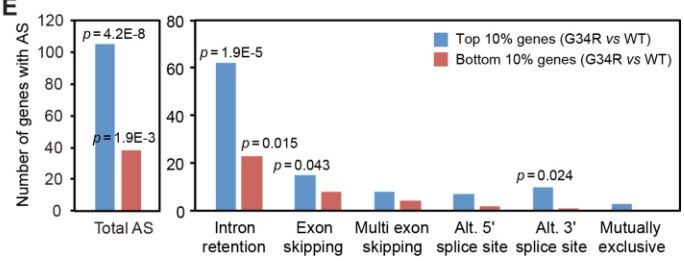

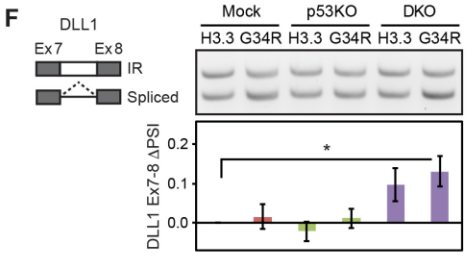

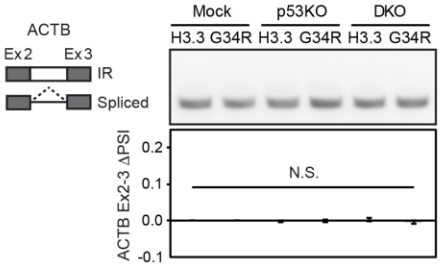

Figure S4. Alternative RNA splicing events impacted by the mutations, related to Figure 4.

(A) Volcano plots show alternative splicing events up- or down-regulated in DKO-G34R cells. (B) Motif analysis shows consensus splice acceptor and donor motifs at the intron retention sites down-regulated in triple-mutant vFNPCs (DKO-G34R). (C) Pathway analysis shows that most genes alternatively spliced in DKO-G34R cells are known targets of AS. (D) Clinical characteristics of H3.3G34R-mutant and age- and location-matched histone-wildtype HGGs used for AS analysis. (E) Bar graph shows overlaps between genes alternatively spliced in H3.3G34R-mutant tumors compared to histone-wildtype tumors (ΔPSI > 10% and p value < 0.05) and genes differentially expressed in H3.3G34R-mutant tumors (top 10% and bottom 10% of genes sorted by the ratio of mean values). (F) RT-PCR confirms the changes of intron retention in *DLL1* in vFNPCs. Band intensity was quantified using Image J and Percentage Spliced In (PSI) values are shown in the bar charts. Bars indicate mean ± S.E.M. (n = 3-5). (G) *ACTB* (ß-actin) was used as a negative control. *P* values were calculated by hypergeometric test (E) or by two-sided paired t-test (F, G). **P* < 0.05. NS, Not Significant. PSI, Percentage Spliced In.

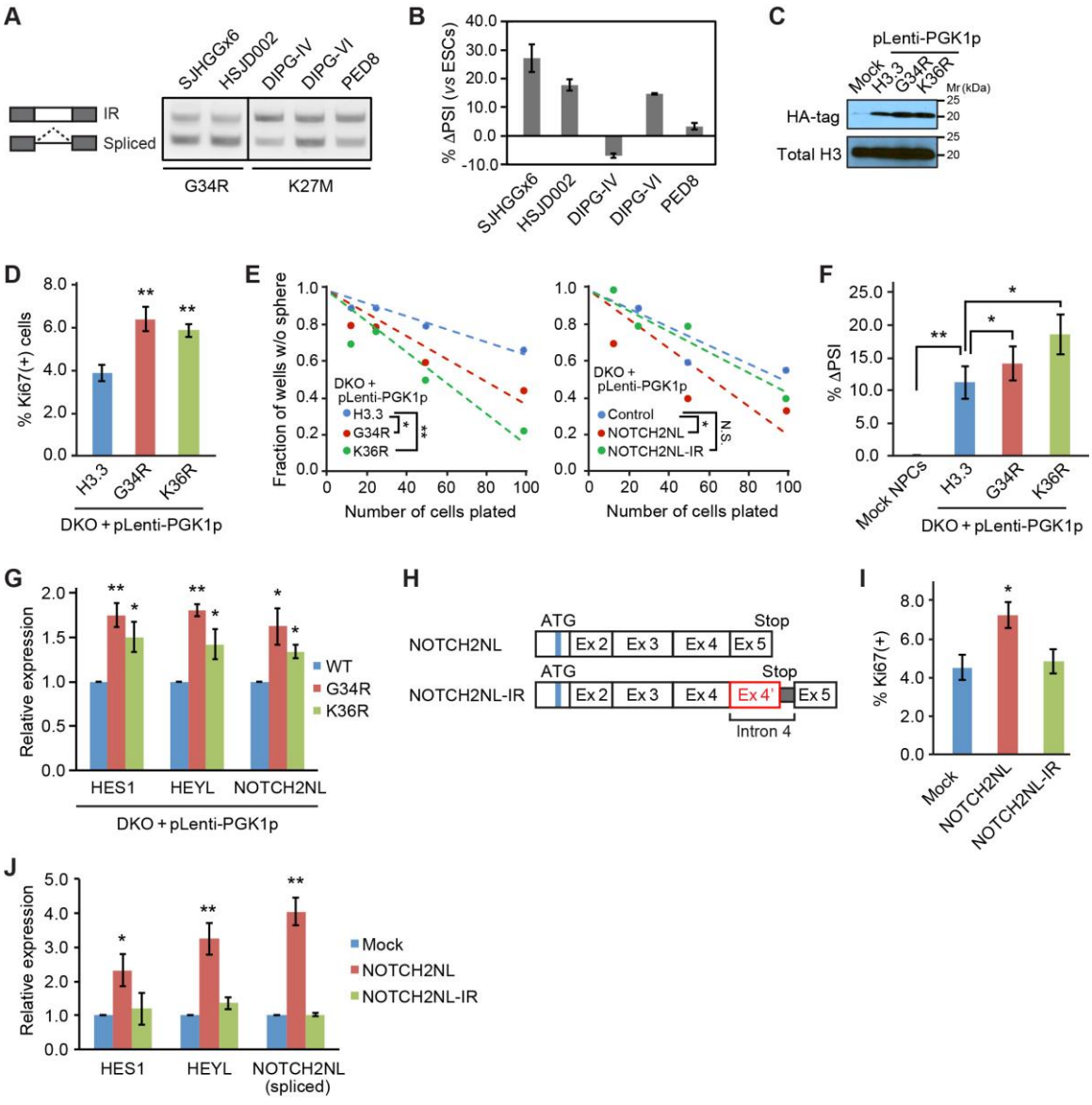
A
SJHGGx6
HSJD002
DIPG-IV
DIPG-VI
PED8
IR
Spliced
G34R
K27M
B
% ΔPSI (vs ESCs)
40.0
30.0
20.0
10.0
0.0
-10.0
SJHGGx6
HSJD002
DIPG-IV
DIPG-VI
PED8
C
pLenti-PGK1p
Mock
H3.3
G34R
K36R
Mr (kDa)
HA-tag
Total H3
25
20
25
20
D
% Ki67(+) cells
8.0
6.0
4.0
2.0
0.0
**
**
H3.3
G34R
K36R
DKO + pLenti-PGK1p
E
Fraction of wells w/o sphere
1.0
0.8
0.6
0.4
0.2
0.0
0
20
40
60
80
100
Number of cells plated
DKO + pLenti-PGK1p
H3.3
G34R
K36R
*
**
DKO + pLenti-PGK1p
Control
NOTCH2NL
NOTCH2NL-IR
*
N.S.
Number of cells plated
F
% ΔPSI
25.0
20.0
15.0
10.0
5.0
0.0
**
*
*
Mock NPCs
H3.3
G34R
K36R
DKO + pLenti-PGK1p
G
Relative expression
2.0
1.5
1.0
0.5
0.0
**
*
**
*
*
*
WT
G34R
K36R
HES1
HEYL
NOTCH2NL
DKO + pLenti-PGK1p
H
NOTCH2NL
ATG
Stop
Ex 2
Ex 3
Ex 4
Ex 5
NOTCH2NL-IR
ATG
Stop
Ex 2
Ex 3
Ex 4
Ex 4'
Ex 5
Intron 4
I
% Ki67(+)
8.0
6.0
4.0
2.0
0.0
*
Mock
NOTCH2NL
NOTCH2NL-IR
J
Relative expression
5.0
4.0
3.0
2.0
1.0
0.0
*
**
**
Mock
NOTCH2NL
NOTCH2NL-IR
HES1
HEYL
NOTCH2NL
(spliced)

Figure S5. Upregulation of the *NOTCH2NL* genes by the mutations, related to Figure 5.

(A) H3.3G34R-mutant tumor cell lines (SJHGGx6 and HSJD002) show lower levels of intron retention of *NOTCH2NL* compared to K27M-mutant tumor cell lines (DIPG-IV, DIPG-VI, PED8). (B) Levels of alternative splicing were quantified by quantitative real-time RT-PCR using primer pairs specifically amplify spliced and unspliced transcripts, respectively. Bars indicate mean ± S.E.M. (n = 3). (C) Western blotting of chromatin fraction shows the expression of the indicated histone transgenes and their chromatin incorporation. (D) Intracellular Flow Cytometry shows an increase of Ki67-positive cells by overexpression of H3.3G34R- and H3.3K36R-mutant transgenes. Bars indicate mean ± S.E.M. (n = 5-6). (E) Limiting dilution assay shows an increase in sphere-forming capacity by overexpression of H3.3G34R- and H3.3K36R-mutant histones (Left panel) or the *NOTCH2NL* transgene (Right panel). Intron-retaining NOTCH2NL (NOTCH2NL-IR) shows no effect on sphere formation. (F) Quantitative RT-PCR shows altered splicing of NOTCH2NL intron 4 by expression of H3.3G34R- and H3.3K36R-mutant histone H3.3 transgenes. Bars indicate mean ± S.E.M. (n = 5). (G) Quantitative RT-PCR shows an increase in the expression of Notch target genes *HES1* and *HEYL*. Bars indicate mean ± S.E.M. (n = 3-4). (H) Schematic illustration of constructs expressing intron-excised and intron-retaining *NOTCH2NL* (NOTCH2NL-IR) transgenes. (I) Intracellular Flow Cytometry shows an increase of Ki67-positive cells by overexpression of *NOTCH2NL*, but not intron-retained *NOTCH2NL*. Bars indicate mean ± S.E.M. (n = 3). (J) Quantitative RT-PCR shows an increase in the expression of Notch target genes *HES1* and *HEYL* by overexpression of *NOTCH2NL*, but not intron-retaining *NOTCH2NL*. Bars indicate mean ± S.E.M. (n = 3). *P* values were calculated by two-sided Welch's t test (D, G, I and J), two-sided paired t-test (F) or by the likelihood-ratio test (E). **P* < 0.05, ***P* < 0.01.

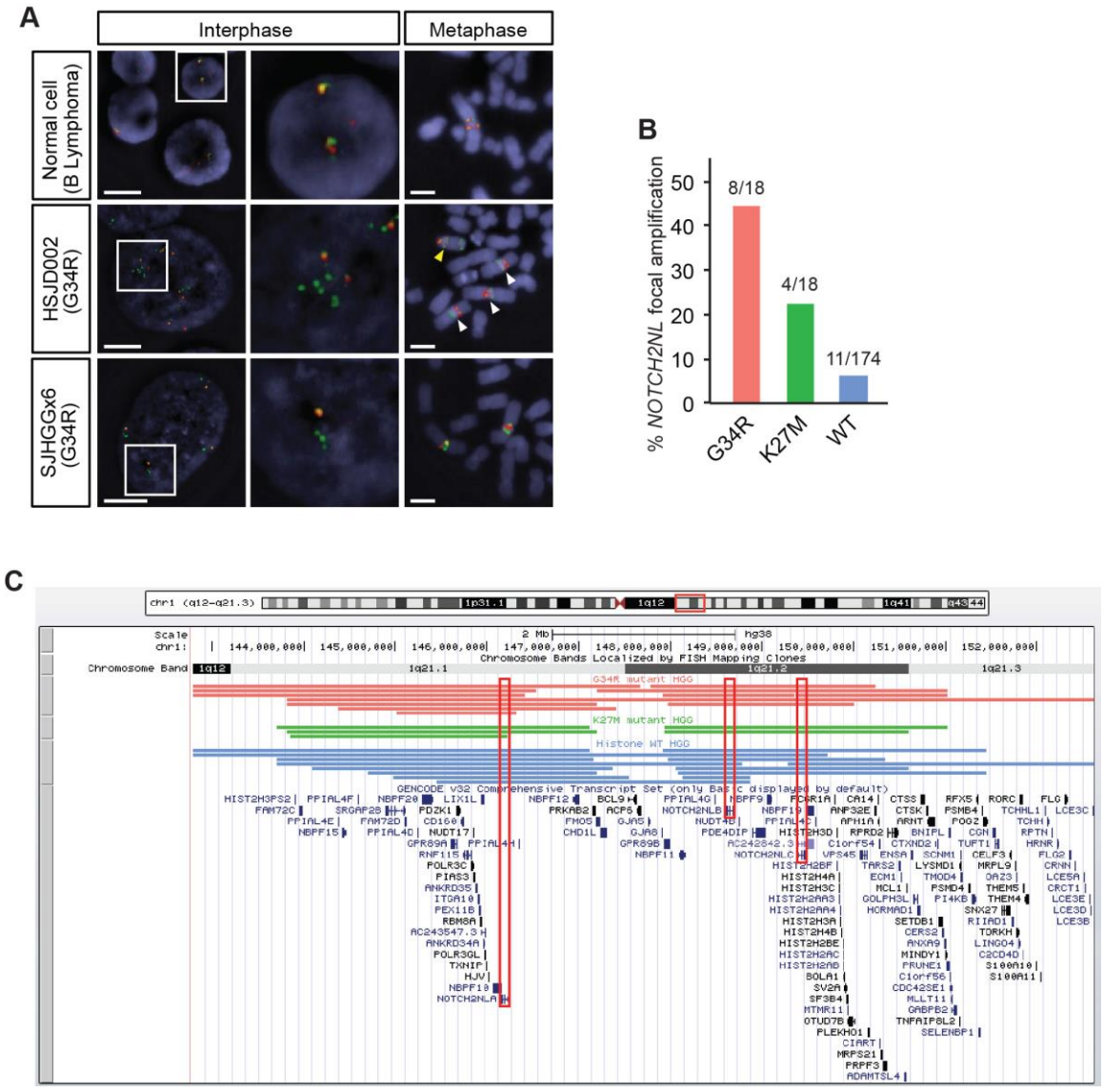

Figure S6. *NOTCH2NL* amplification in H3.3G34R-mutant HGGs, related to Figure 6.

(A) Fluorescent *in situ* hybridization (FISH) confirmed genomic amplification of *NOTCH2NL* locus (green) in two H3.3G34R-mutant patient-derived cell lines. FISH probe targeting *NOTCH2* locus is shown in red. Immortalized B lymphoma cells were used as control. Scale bar, 5 μm. (B) The percentage ratio of tumors with *NOTCH2NL* focal amplification is shown for each tumor type (n = 210). (C) Focal amplifications associated with *NOTCH2NL* genes in each tumor type are mapped to the human genome (hg38).

Table S1. Oligonucleotide sequences, related to STAR Methods

Primer sequences for RT-qPCR	
HES1_Fw	ACGACACCGGATAAACCAAA
HES1_Rv	TCAGCTGGCTCAGACTTTCA
ASCL1_Fw	AGTTGGTCAACCTGGGCTTT
ASCL1_Rv	AGCGCAGTGTCTCCACCTTA
HEYL_Fw	AGACCGCATCAACAGTAGCC
HEYL_Rv	TTTCAAGTGATCCACCGTCA
TP53/p53_Fw	AGGCCTTGGAACTCAAGGAT
TP53/p53_Rv	TTATGGCGGGAGGTAGACTG
CDKN1A/p21_Fw	GGAGACTCTCAGGGTCGAAA
CDKN1A/p21_Rv	GGATTAGGGCTTCCTCTTGG
ATRX_Fw	GACACCCTTCATTGCAAGTTC
ATRX_Rv	TTCCATCTGAGTCACGGCTA
NOTCH2NL_Fw	GGCAGACTGGTGACTTCACTT
NOTCH2NL_Rv	TCGTGTTCTTTTCCATTCCAG
FOXG1_Fw	CAACGGCATCTACGAGTTCA
FOXG1_Rv	TGTTGAGGGACAGATTGTGG
SP8_Fw	GAGAGGAGGAGGGCACTTTT
SP8_Rv	GCTGGGGCTGCCTATCTTAT
ARX_Fw	GACACCCAGCTTTCATCAGC
ARX_Rv	GGTGTGGGCTGTCTCAGG
NKX6-1_Fw	ACACGAGACCCACTTTTTCCG
NKX6-1_Rv	TGCTGGACTTGTGCTTCTTCAAC
HOXB2_Fw	TCTCCCCTAGCCTACAGGGTTC
HOXB2_Rv	GGTGAAAAAATCCAGCTCTTCCT
DLX1_Fw	GGTTCCAGCAAACTCAGTACCT
DLX1_Rv	CTTGAACTTGGATCGCTTGTTT
DLX2_Fw	CCCTATGGAACCAGTTCGTC
DLX2_Rv	TTGGCTTCCCGTTCACTATC
ID1_Fw	CCTCAACGGCGAGATCAG
ID1_Rv	CGCTTCAGCGACACAAGA
ACTB_Fw	GTCATTCCAAATATGAGATGCGT
ACTB_Rv	GCTATCACCTCCCCTGTGTG
Primer sequences for RT-PCR (Alternative Splicing)	
NOTCH2NL_Exon4_Fw	TCTCCTGCAAATGCCTCAC
NOTCH2NL_Exon5_Rv	TACTCCATCAAAAGCAAAAGCA
DLL3_Exon7_Fw	GTAGATTGGAATCGCCCTGA
DLL3_Exon8_Rv	AGAGAGATGGGGTGAGAAAAA
DLL1_Exon7_Fw	ATAAGCCCTGCAAGAATGGA
DLL1_Exon8_Rv	CAGGGTGAAGAGCTGCAGTA
ACTB_Exon2_Fw	AAGACCTGTACGCCAACACA
ACTB_Exon3_Rv	AAAGCCATGCCAATCTCATC
Primer sequences for qRT-PCR (Alternative Splicing)	
NOTCH2NL_spliced_Fw	CTGCCTTCCAGAAACAGTGAG
NOTCH2NL_spliced_Rv	CATCGTGTTCTTTTCCATTCC
NOTCH2NL_IR_Fw	TGCAACTGCCTTCCAGGT
NOTCH2NL_IR_Rv	ACACCCACTACCTCCTGTGCT
DLL3_spliced_Fw	GAGCTCGTCCGTAGATTGGA
DLL3_spliced_Rv	AGGCCTCCCGAGCGTAGA
DLL3_IR_Fw	GCCAGAGCTTTTCCACTGAT

DLL3_IR_Rv	GCGTCAGGCCTAGAAACAAA
Primer sequences for ChIP-PCR	
NOTCH2NL_pair1_Fw	CCTCGGTCCTTCTCTGTGTG
NOTCH2NL_pair1_Rv	ATGTCCAAACTCTCGGGAAC
NOTCH2NL_pair2_Fw	TGCAACTGCCTTCCAGGT
NOTCH2NL_pair2_Rv	ACACCCACTACCTCCTGTGCT
LHX8_1st_Intron_Fw	AGAGAAAGGGCCTCAACTCC
LHX8_1st_Intron_Rv	ACACTTTCTCATCGCCTGCT
Primer sequences for genomic PCR	
NOTCH2NL_Fw	CACTCTGCGGTGGCAGTA
NOTCH2NL_Rv	CCACCTTTCAGGTCCTAACATT
NOTCH2+NL_Fw	GCCTAGTCACACCAAATTCTCC
NOTCH2+NL_Rv	GTTGTAGAAAAGGGCATTCCAG
GAPDH_TSS_Fw	AATTCCCCATCTCAGTCGTTC
GAPDH_TSS_Rv	CAGCAGGACACTAGGGAGTCA
shRNA target sequences	
shNOTCH2NL #1	GAGCTCTGGGAAAGAGACAGG
shNOTCH2NL #2	GGTTAATAAAGTGCTTTAAAC